

Thermal transport properties of polycrystalline tin-doped indium oxide films

Toru Ashida,^{1,a)} Amica Miyamura,¹ Nobuto Oka,¹ Yasushi Sato,¹ Takashi Yagi,² Naoyuki Taketoshi,² Tetsuya Baba,² and Yuzo Shigesato^{1,b)}

¹Graduate School of Science and Engineering, Aoyama Gakuin University, 5-10-1 Fuchinobe, Sagamihara, Kanagawa 229-8558, Japan

²National Metrology Institute of Japan, National Institute of Advanced Industrial Science and Technology (AIST), Tsukuba Central 3, 1-1-1 Umezono, Tsukuba, Ibaraki 305-8563, Japan

(Received 22 October 2008; accepted 28 January 2009; published online 13 April 2009)

Thermal diffusivity of polycrystalline tin-doped indium oxide (ITO) films with a thickness of 200 nm has been characterized quantitatively by subnanosecond laser pulse irradiation and thermorefectance measurement. ITO films sandwiched by molybdenum (Mo) films were prepared on a fused silica substrate by dc magnetron sputtering using an oxide ceramic ITO target (90 wt % In₂O₃ and 10 wt % SnO₂). The resistivity and carrier density of the ITO films ranged from 2.9×10^{-4} to 3.2×10^{-3} Ω cm and from 1.9×10^{20} to 1.2×10^{21} cm⁻³, respectively. The thermal diffusivity of the ITO films was $(1.5\text{--}2.2) \times 10^{-6}$ m²/s, depending on the electrical conductivity. The thermal conductivity carried by free electrons was estimated using the Wiedemann–Franz law. The phonon contribution to the heat transfer in ITO films with various resistivities was found to be almost constant ($\lambda_{\text{ph}}=3.95$ W/m K), which was about twice that for amorphous indium zinc oxide films. © 2009 American Institute of Physics. [DOI: 10.1063/1.3093684]

I. INTRODUCTION

Polycrystalline tin-doped indium oxide (ITO) thin films have been widely used as transparent conductive electrodes (TCE) in various optoelectronic applications such as liquid crystal displays, plasma displays, solar cells, and organic electroluminescence diodes, because they possess high electrical conductivity and high optical transparency in the visible region. Although the several methods have been employed for the deposition process of ITO thin films, dc magnetron sputtering using a ceramic ITO target is the most preferred method because of the advantages of controllability of sputtering conditions and adaptability to large-area deposition.¹

The thermophysical properties of transparent conductive electrodes received a lot of attention recently since heat generation in a circuit should increase the likelihood of a short circuit or overheating, which would damage the flat panel displays. We already reported thermal diffusivity measurements for indium zinc oxide (IZO) thin films with a thickness of 200 nm conducted using the nanosecond thermorefectance technique.² The thermal diffusivity of IZO films ranged from 6.3×10^{-7} to 1.4×10^{-6} m²/s, depending on the electrical conductivity, and the thermal conductivity carried by phonons should be almost constant for all degenerated IZO films ($\lambda_{\text{ph}}=1.85$ W/m K). However, there have been no detailed studies on polycrystalline ITO thin films to date even though they are the key material in flat panel displays.

The carrier density n of polycrystalline ITO films is dominated by the oxygen vacancy concentration and electri-

cally activated substitutional Sn⁴⁺ at the In³⁺ site, which can be easily controlled over the wide range from 10^{19} to above 10^{21} cm⁻³ by adjusting the deposition conditions.^{3,4} Thus, it is important to characterize the thermophysical properties of ITO films and examine how these depend on their electrical properties in order to determine the heat propagation mechanisms in polycrystalline conductive ceramics.

In this study, polycrystalline ITO films with various electrical properties were deposited. In order to measure the thermal diffusivity of submicron-thick ITO films quantitatively, a newly developed novel thermorefectance measurement apparatus was employed, whose geometrical configuration was quite similar to that of a conventional laser flash apparatus used for bulk thermal diffusivity measurements.^{2,5} This apparatus was developed on the basis of the picosecond thermorefectance system developed by the National Metrology Institute of Japan/AIST.^{6,7} A nanosecond pulsed pump laser and a subnanosecond pulsed probe laser are used in order to measure the heat propagation caused by pulse heating through the film thickness. The relationships between electrical and thermophysical properties of the ITO films were analyzed in detail. The thermal transport mechanisms in the polycrystalline transparent conductive oxide were discussed.

II. EXPERIMENTAL

ITO films sandwiched by molybdenum films (Mo/ITO/Mo) were prepared on unheated fused silica glass substrates by dc magnetron sputtering with a power of 50 W using an oxide ceramic In₂O₃–SnO₂ target (90.0 wt % In₂O₃ and 10.0 wt % SnO₂, Tosoh Corp.) and Mo metal target, respectively. The substrate temperature during deposition was confirmed to be below 50 °C by the thermolabel. All the as-deposited films were postannealed in Ar (100%) for 1 h at

^{a)}Present address: Glass Research Center, Central Glass Co., Ltd., 1510 Ohkuchi-Cho, Matsusaka City, Mie Prefecture, 515-0001, Japan.

^{b)}Author to whom correspondence should be addressed. Electronic mail: yuzo@chem.aoyama.ac.jp.

200 °C using a tube type furnace. The ITO layers were deposited under varying oxygen flow rates between 0% and 5%. The water partial pressure of the residual gas was maintained below 7×10^{-4} Pa and the total gas pressure (P_{tot}) of Ar, Ar+O₂, was kept at 0.7 Pa for all deposition runs. Mo layers were deposited at $P_{\text{tot}}=0.7$ Pa of 100% Ar. The Mo/ITO/Mo layered structure was fabricated without exposure to the atmosphere between each deposition. The nominal thickness of the ITO layer was 200 nm. Mo layers with a thickness of 70 nm were necessary because the wavelengths of pulse laser used in this study are 785 and 1064 nm, at which wavelength ITO films are transparent.

A pump laser pulse with a wavelength of 1064 nm and a pulse width of 800 ps was focused on the surface of the Mo/ITO/Mo specimen with a spot diameter of 300 μm and an optical power of 50 mW. The partial energy of the pump laser pulse was absorbed into skin depth of the bottom Mo layer and converted into heat. Then, the heat propagated through the specimen thickness. A probe laser pulse with a wavelength of 785 nm and a pulse width of 150 ps detected the temperature change at the opposite side of the Mo/ITO/Mo layers as change in reflectivity. The temperature history at the surface by backside pulse heating was recorded as a function of the delay time relative to the pump laser pulse. To derive the thermal diffusivity of the ITO thin films, the thermoreflectance signals were analyzed on the basis of an analytical solution of the one-dimensional heat flow across the three-layered film/substrate system.⁸

In order to characterize its structural, electrical, and optical properties, the ITO monolayer was also deposited directly on unheated fused silica substrate and postannealed at 200 °C in Ar. The film thickness was measured using a surface profiler (Dektak³, Sloan Tech.). The electrical resistivity (ρ) and free carrier density (n) of the films were analyzed by the four-point probe method and Hall-effect measurement in the van der Pauw geometry (HL-550PC, Bio-Rad). For the ITO films deposited at 100% Ar, the temperature dependence of ρ and n was analyzed over the temperature range from 100 to 300 K. X-ray diffraction (XRD) was carried out by 40 kV, 20 mA Cu $K\alpha 1$ radiation (XRD-6000, Shimadzu). Transmittance and reflectance of the films were measured from 190 to 2500 nm using a spectrophotometer (UV-3100, Shimadzu). A nanoindenter equipped with a Berkovich diamond indenter (ENTO-1100, ELIONIX) was used to measure Young's modulus.

III. RESULTS

A. Structure of ITO films

Figure 1 shows XRD patterns of postannealed ITO films deposited on fused silica glass substrates at various oxygen flow ratios. All the ITO films showed a bixbyite In₂O₃ polycrystalline structure, which was confirmed by the XRD peaks of the (211), (222), (400), (440), and (622) planes.

B. Electrical and optical properties of ITO films

The electrical resistivity (ρ) and free carrier density (n) of ITO films are shown in Table I as a function of O₂ flow ratio during the depositions. As is typical for a highly degen-

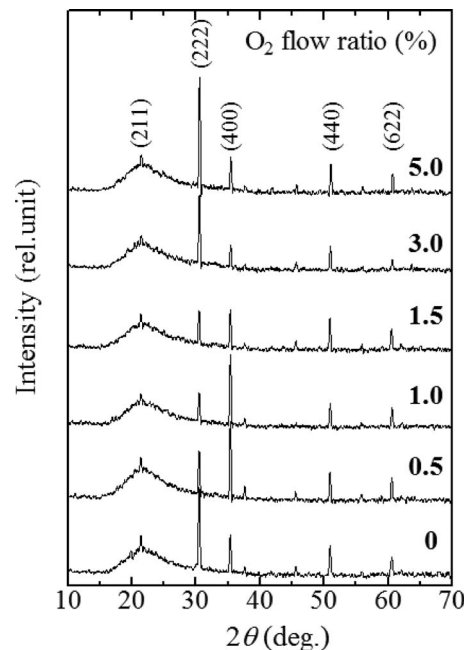


FIG. 1. XRD patterns of ITO films deposited under various oxygen flow ratios [O₂/(Ar+O₂)]. The halo pattern observed around $2\theta=20^\circ-25^\circ$ was from the glass substrate.

erate semiconductor,^{9,10} these films showed almost a constant in ρ and n over the temperature range from 100 to 300 K.

On the other hand, all the ITO films in this study exhibited a high transmittance of over 80% in the visible range. The transmittance in the near-infrared region (wavelength >1000 nm) decreased with increasing n , while the reflectance increased. These variations can be explained by the Drude theory.^{9,11}

C. Thermal diffusivity of ITO films

Figure 2 shows the typical thermoreflectance signals of Mo/ITO/Mo three-layered films. The gas flow ratios during the ITO depositions were 0% and 5% O₂. We note that the intensity of the thermoreflectance signal increases linearly with temperature¹² and the shape of these curves imply a temperature history similar to that obtained by the conventional laser flash method for a bulk material.¹³ Thus, the larger thermal diffusivity of the layer causes a more rapid signal rise. The thermal diffusivity of the ITO films was analyzed on the basis of a previously reported one-dimensional heat flow model for three-layered films.⁸ For this analysis, a Mo film thickness (d_{Mo}) of 70 nm, a thermal diffusivity

TABLE I. Resistivity (ρ) and carrier density (n) for ITO thin films as a function of O₂ flow ratios during the depositions.

| O ₂ flow ratio (%) | ρ (Ω cm) | n (cm^{-3}) |
|-------------------------------|-----------------------|--------------------------|
| 0 | 3.8×10^{-4} | 1.2×10^{21} |
| 0.5 | 2.9×10^{-4} | 1.1×10^{21} |
| 1.0 | 5.1×10^{-4} | 7.4×10^{20} |
| 1.5 | 5.2×10^{-4} | 5.6×10^{20} |
| 3.0 | 2.6×10^{-3} | 2.2×10^{20} |
| 5.0 | 3.2×10^{-3} | 1.9×10^{20} |

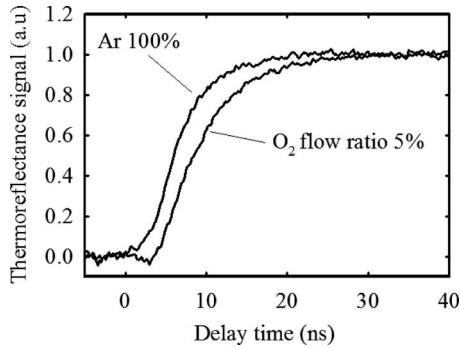


FIG. 2. Thermoreflectance signals of the Mo/ITO/Mo three-layered thin films deposited under 100% Ar. An O₂ flow ratio of 5% obtained by the nanosecond thermoreflectance measurements.

(κ_{Mo}) of $2.0 \times 10^{-5} \text{ m}^2 \text{ s}^{-1}$, a heat capacity per unit volume (C_{Mo}) for Mo of $2.53 \times 10^6 \text{ J m}^{-3} \text{ K}^{-1}$, and a heat capacity per unit volume (C_{ITO}) for ITO of $2.58 \times 10^6 \text{ J m}^{-3} \text{ K}^{-1}$ were used,^{8,14} where the value of $C_{\text{In}_2\text{O}_3}$ was used for C_{ITO} . In addition, the thermal resistances at the interface between the layers were neglected in this study because a boundary thermal resistance of this type was reported to be about 10^{-9} – $10^{-8} \text{ m}^2 \text{ K/W}$, which was much smaller than the total thermal resistance of the films.⁸

Figure 3 shows the thermal diffusivity of ITO films in relation to O₂ flow ratios during the depositions. The thermal diffusivity of an ITO film deposited under 100% Ar gas was $2.24 \times 10^{-6} \text{ m}^2/\text{s}$. This thermal diffusivity value was about twice that for amorphous ITO and IZO films.^{2,8} The thermal diffusivity increased to a maximum value of $2.27 \times 10^{-6} \text{ m}^2/\text{s}$ with the slight increase in the O₂ flow ratio of up to 0.5% and then decreased sharply to $1.53 \times 10^{-6} \text{ m}^2/\text{s}$ with a further increase in the O₂ flow ratio.

IV. DISCUSSION

As shown in Table I, the electrical properties of ITO thin films changed dramatically with increasing O₂ flow ratio. In the case of carrier densities above $1 \times 10^{20} \text{ cm}^{-3}$, the ITO films are highly degenerate, where free electrons behave like those in a metal. Accordingly, the mechanism of thermal transport in ITO films must be discussed in terms of both contributions of free electrons and phonons. It is well known

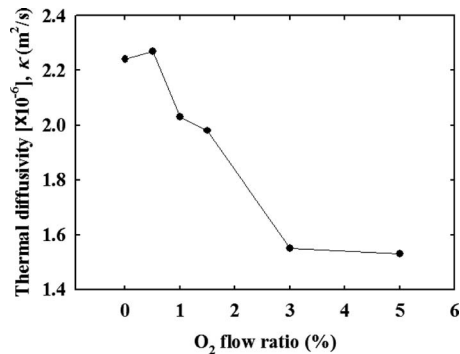


FIG. 3. Thermal diffusivity of ITO films as a function of O₂ flow ratio during the depositions.

TABLE II. Electrical conductivity (σ), thermal conductivity (λ), and electrical contribution to thermal conductivity (λ_{el}) for ITO thin films estimated from the Wiedemann–Franz law.

| O ₂ flow ratio (%) | σ (Sm ⁻¹) | λ (W m ⁻¹ K ⁻¹) | $\lambda_{\text{el}}/\lambda$ |
|-------------------------------|------------------------------|--|-------------------------------|
| 0 | 2.6×10^5 | 5.86 | 0.32 |
| 0.5 | 3.4×10^5 | 5.95 | 0.42 |
| 1.0 | 2.0×10^5 | 5.31 | 0.27 |
| 1.5 | 1.9×10^5 | 5.19 | 0.26 |
| 3.0 | 3.9×10^4 | 4.06 | 0.07 |
| 5.0 | 3.0×10^4 | 4.00 | 0.05 |

that the thermal conductivity carried by free electrons λ_{el} can be described in terms of the electrical conductivity σ by the Wiedemann–Franz law,

$$\lambda_{\text{el}} = LT\sigma, \quad (1)$$

where L is the Lorentz number ($2.45 \times 10^{-8} \text{ W } \Omega/\text{K}^2$) and T is the absolute temperature. On the basis of Eq. (1), the λ_{el} values for ITO films were estimated using σ (see Table II), where the total thermal conductivity, λ , was derived from the measured thermal diffusivity using the density and specific heat capacity of the bulk In₂O₃ crystal. The contribution of free electrons to the thermal conductivity reached 40% of the total thermal conductivity for highly degenerate ITO films.

The thermal conductivity of ITO films is plotted as a function of σ in Fig. 4, where the value for the amorphous IZO film is also plotted for comparison.² The dashed line represents the calculated λ_{el} determined by the Wiedemann–Franz law. By subtracting λ_{el} from the measured total thermal conductivity, the thermal conductivity carried by phonons, λ_{ph} , can be estimated. The slope of the plot of total thermal conductivity versus σ seems to be equal to that of λ_{el} . Thus, λ_{ph} should be almost constant for all the degenerate ITO films examined in this study, where the value of λ_{ph} is about 3.95 W/mK. On the other hand, λ_{ph} for the amorphous IZO is half that for the ITO films. Consequently, the phonon propagation in the polycrystalline ITO films clearly differs from that in the amorphous IZO films.

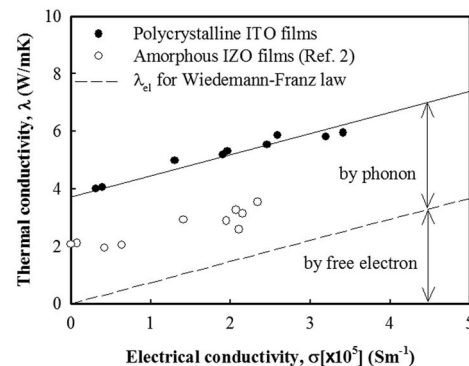


FIG. 4. Thermal conductivity vs electrical conductivity for ITO films deposited at various O₂ flow ratios. The thermal conductivity calculated using the Wiedemann–Franz law is also shown by a dotted line. For comparison, the thermal conductivity of the amorphous IZO film is also plotted by open circles (Ref. 2).

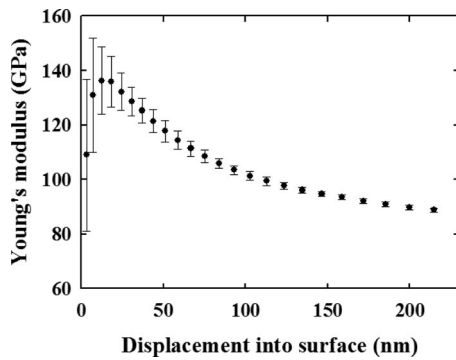


FIG. 5. Young's modulus of the polycrystalline ITO film with a thickness of 200 nm obtained by a nanoindenter.

As mentioned earlier, the thermal conductivity due to phonons λ_{ph} for the ITO films was constant, suggesting that the mean free path of phonons l_{ph} should be almost constant for ITO films deposited under various conditions in this study. Thus, it is of interest to estimate the effective structure size of phonon propagation in ITO in terms of l_{ph} . λ_{ph} is described via the following equation:

$$\lambda_{\text{ph}} = \frac{1}{3} C v l_{\text{ph}}, \quad (2)$$

where C is the heat capacity per unit volume, and v , the average phonon velocity, is calculated from the Young's modulus E and density ρ_d through the following equation:¹⁵

$$v = \left(\frac{E}{\rho_d} \right)^{1/2}. \quad (3)$$

Figure 5 shows the Young's modulus of polycrystalline ITO films with a thickness of 200 nm. The Young's modulus for ITO films was 134.9 GPa, which adopted this value at a depth of 20 nm taking into account the influence of surface and substrate. Thus, λ_{ph} can be calculated using Eqs. (2) and (3) with the values given in Table III.

The l_{ph} of the polycrystalline ITO films is estimated to be 0.99 nm (Table III). The lattice constant of bixbyite In_2O_3 (1.0118 nm) was reported.¹¹ It can be concluded that the l_{ph} of the polycrystalline ITO films is of the order of the lattice constant. In the case of the amorphous IZO film, l_{ph} was 0.40 nm.² This is smaller than the value for the polycrystalline ITO films, but almost twice the single In–O bond length.¹⁶

TABLE III. The phonon mean free path (l_{ph}) calculated using the density of In_2O_3 (ρ_d) (Ref. 11), Young's modulus (E), and average phonon velocity (v). For comparison, the l_{ph} for the amorphous IZO films is also shown (Ref. 2).

| Materials | λ_{ph} ($\text{W m}^{-1} \text{K}^{-1}$) | ρ_d (10^3 kg m^{-3}) | E (GPa) | v (ms^{-1}) | l_{ph} (nm) |
|-----------|--|--|--------------|-----------------------------|-------------------------|
| ITO | 3.95 | 7.12 | 134.9 | 4354 | 0.99 |
| IZO | 1.85 | 7.12 | 141.0 | 4430 | 0.40 |

V. CONCLUSIONS

The thermal diffusivity of 200-nm-thick polycrystalline ITO films with widely varying electrical conductivities was investigated by the nanosecond thermoreflectance method. Three-layered specimens that consisted of a polycrystalline ITO film sandwiched by 70-nm-thick Mo films (Mo/ITO/Mo) were fabricated on fused silica substrates by dc magnetron sputtering. During the deposition of the ITO film, Ar–O₂ mixture gases were used in order to control the electrical conductivity of the ITO films. Thermal diffusivity of the ITO films ranged from 2.3×10^{-6} to $1.5 \times 10^{-6} \text{ m}^2/\text{s}$, which was associated with the electrical conductivity of the films via the Wiedemann–Franz law. The contribution of free electrons to the thermal conductivity reached 40% of the total thermal conductivity for the highly degenerate ITO films. The mean free path of phonons in the ITO films was estimated to be 0.99 nm, which coincides with the lattice constant of bixbyite In_2O_3 .

ACKNOWLEDGMENTS

The author would like to thank Y. Seino of the National Institute of Advanced Industrial Science and Technology (AIST) for the Young's modulus analyses. This work was partially supported by a High-Tech Research Center project for private universities with the matching fund subsidy from the Ministry of Education, Culture, Sports, Science and Technology (MEXT) of the Japanese Government.

- ¹R. Latz, K. Michael, and M. Scherer, *Jpn. J. Appl. Phys., Part 2* **30**, L149 (1991).
- ²T. Ashida, A. Miyamura, Y. Sato, T. Yagi, N. Taketoshi, T. Baba, and Y. Shigesato, *J. Vac. Sci. Technol. A* **25**, 1178 (2007).
- ³G. Frank and H. Köstlin, *Appl. Phys. A: Solids Surf.* **27**, 197 (1982).
- ⁴Y. Sato, R. Tokumaru, E. Nishimura, P. K. Song, Y. Shigesato, K. Utsumi, and H. Iigusa, *J. Vac. Sci. Technol. A* **23**, 1167 (2005).
- ⁵T. Baba, Proceedings of the Tenth International Workshop on Thermal Investigations of ICs and Systems, Sophia Antipolis, France, 2004 (unpublished).
- ⁶N. Taketoshi, T. Baba, E. Schaub, and A. Ono, *Rev. Sci. Instrum.* **74**, 5226 (2003).
- ⁷N. Taketoshi, T. Baba, and A. Ono, *Rev. Sci. Instrum.* **76**, 094903 (2005).
- ⁸T. Yagi, K. Tamano, Y. Sato, N. Taketoshi, T. Baba, and Y. Shigesato, *J. Vac. Sci. Technol. A* **23**, 1180 (2005).
- ⁹Y. Shigesato, D. C. Paine, and T. E. Haynes, *J. Appl. Phys.* **73**, 3805 (1993).
- ¹⁰Y. Shigesato, N. Shin, M. Kamei, P. K. Song, and I. Yasui, *Jpn. J. Appl. Phys., Part 1* **39**, 6422 (2000).
- ¹¹I. Hamberg and C. G. Granqvist, *J. Appl. Phys.* **60**, R123 (1986).
- ¹²N. Taketoshi, T. Baba, and A. Ono, *Jpn. J. Appl. Phys., Part 2* **38**, L1268 (1999).
- ¹³W. J. Parker, R. J. Jenkins, and G. L. Abbot, *J. Appl. Phys.* **32**, 1679 (1961).
- ¹⁴I. Barin and G. Platzki, *Thermochemical Data of Pure Substances* (VCH, Weinheim, 1995).
- ¹⁵C. Kittel, *Introduction to Solid State Physics*, 7th ed. (Wiley, New York, 1996), pp. 98–101.
- ¹⁶F. Utsuno, H. Inoue, Y. Shimane, T. Shibuya, K. Yano, K. Inoue, I. Hiro-sawa, M. Sato, and T. Honma, *Thin Solid Films* **516**, 5818 (2008).